A Hydrophilic Channel Is Involved in Oxidative Inactivation of a [NiFeSe] Hydrogenase

Sónia Zacarias, Adriana Temporão, Melisa Del Barrio, Vincent Fourmond, Christophe Léger, Pedro Matias, Inês Cardoso Pereira

SUPPORTING INFORMATION

A Hydrophilic Channel is Involved in Oxidative Inactivation of a [NiFeSe] Hydrogenase

Sónia Zacarias[1], Adriana Temporão[1], Melisa del Barrio[2], Vincent Fourmond[2], Christophe Léger[2], Pedro M Matias[1,3*], Inês A C Pereira[1*]

[1] Instituto de Tecnologia Química e Biológica António Xavier, Universidade Nova de Lisboa, Av. da República, 2780-157 Oeiras, Portugal

[2] Aix Marseille Univ., CNRS, Bioénergétique et Ingénierie des Protéines, 13402 Marseille CEDEX 09, France.

[3] iBET, Instituto de Biologia Experimental e Tecnológica, Apartado 12, 2780-901 Oeiras, Portugal

Corresponding authors

*matias@itqb.unl.pt

*ipereira@itqb.unl.pt

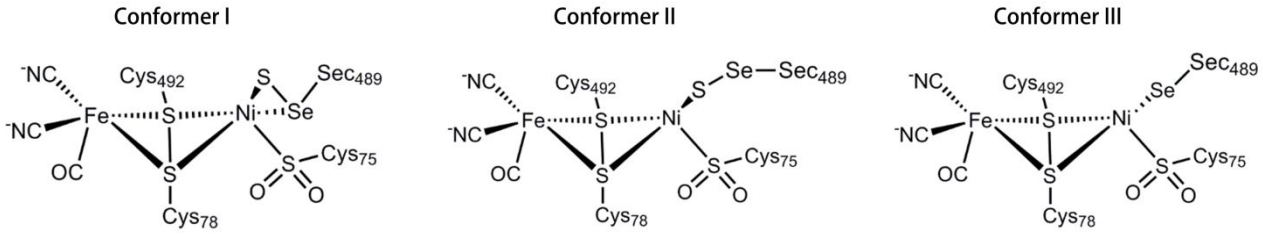

Figure S1. Active site conformations of the as-isolated *D. vulgaris* Hildenborough [NiFeSe] hydrogenase. In conformer I and II an exogenous sulfur is bound to Ni, while in conformer III no exogenous sulfur is present and Se atom is bond directly to Ni. The latter corresponds to the conformer found in the reduced form of the enzyme.

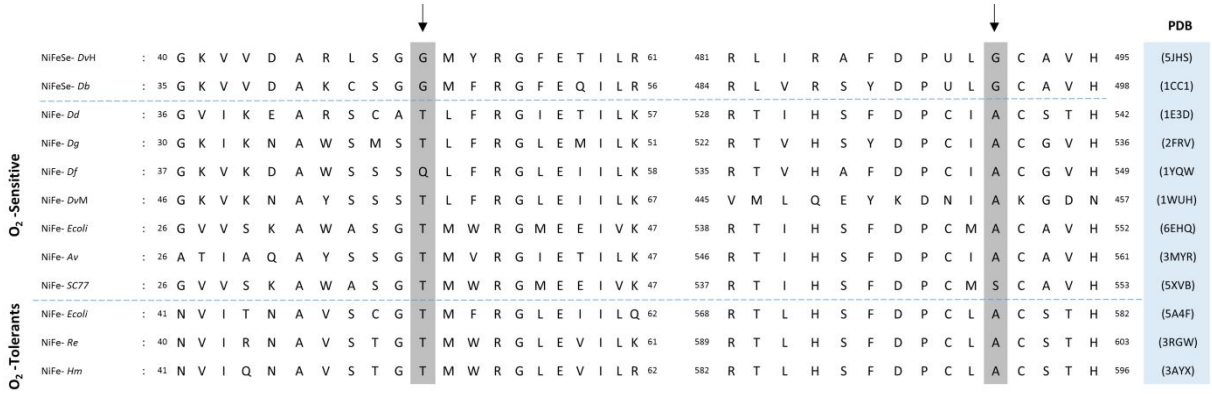

Figure S2. Structure-based sequence alignment of the large subunits of [NiFeSe] hydrogenases from *D. vulgaris* Hildenborough and *D. baculatum* with the standard O_2-sensitive [NiFe] hydrogenases from *D. desulfuricans* ATCC 27774, *D. gigas*, *D. fructosovorans*, *D. vulgaris* Miyazaki, *E. coli*, *Allochromatium vinosum* and *Citrobacter sp.* S-77 with the [NiFe] O_2-tolerant hydrogenases from *E.coli* Hyd-1, *Ralstonia eutropha* and *Hydrogenovibrio marinus.*

Table S1. Data collection and processing statistics

	G50T	***G491A***	***G491S***
Data Collection			
Beamline	ESRF ID29	DLS I02	ESRF ID30A-3
Detector	PILATUS3 6M	PILATUS 6M-F	PILATUS 6M
Wavelength (Å)	0.88560	0.97949	0.88560
Space Group	*C* 2	*P* 2_1	*C* 2
Unit cell parameters:			
a, b, c (Å)	106.18, 62.68, 110.30	60.45, 98.66, 63.88	105.41, 63.59, 110.70
β (°)	105.10	105.36	104.88
Data Processing [a]	AutoPROC / STARANISO	AutoPROC / STARANISO	XDS/CCP4
Resolution limits of ellipsoid fitted to resolution cut-off surface (Å)	1.084, 1.218, 1.223	1.36, 1.56, 1.54	-
Resolution, spherical limits (Å)	53.2-1.084 (1.199-1.084)	61.6-1.36 (1.51-1.36)	45.7-1.20 (1.22-1.20)
Nr. Observations	972918 (45622)	329698 (14355)	1414791 (50213)
Unique reflections	213931 (10698)	112189 (5610)	216144 (9023)
Multiplicity	4.5 (4.3)	2.9 (2.6)	6.5 (5.6)
Completeness, spherical (%)	72.5 (14.0)	71.9 (13.1)	97.9 (83.0)
Completeness, ellipsoidal (%)	90.9 (52.5)	92.7 (52.7)	-
R-merge (%) [b]	11.1 (87.1)	6.2 (58,9)	10.1 (133)
R-p.i.m. (%) [c]	5.9 (46.0)	4.3 (43.7)	4.2 (60.0)
<I/σ (I)>	6.9 (1.6)	10.9 (1.5)	9.4 (1.2)
CC $^{1/2}$	0.992 (0.575)	0.996 (0.613)	0.999 (0.509)
Wilson B (Å²)	10.3	17.6	8.6
Z [d]	1	1	1
Estimated V_M [e]	2.02	2.10	2.05
Estimated Solvent Content (%) [e]	39.2	41.4	40.0

[a] Values in parentheses refer to the highest resolution shell; [b] R-merge = merging R-factor, $(\Sigma_{hkl} \Sigma_i |I_i(hkl) - \langle I(hkl)\rangle|) / (\Sigma_{hkl} \Sigma_i I(hkl)) \times 100$ %; [c] R-p.i.m. = precision-independent R-factor, $\Sigma_{hkl} [1/(N-1)]^{1/2} \Sigma_i |I_i(hkl) - \langle I(hkl)\rangle| / (\Sigma_{hkl} \Sigma_i I_i(hkl)) \times 100$ %.[1] For each unique Bragg reflection with indices (hkl), I_i is the i-th observation of its intensity and N its multiplicity; [d] Nr. molecules in the asymmetric unit; [e] According to Matthews 1968.[2]

Table S2. Refinement statistics

Dataset	G50T	G491A	G491S
Resolution limits (Å) [a]	53.2-1.10 (1.11-1.10)	49.3-1.36 (1.37-1.36)	45.7 1.20 (1.21-1.20)
R_{work} [b]	0.139 (0.318)	0.143 (0.272)	0.128 (0.286)
R_{free} [c]	0.158 (0.329)	0.162 (0.310)	0.148 (0.297)
ML coordinate error estimate (Å) [d]	0.12	0.12	0.12
Model composition and completeness			
Regions omitted [e]	--	1A-6A, 12B-13B	12B
Non-hydrogen protein atoms [f]	6099	5853	6018
Ligand/ion atoms	45	45	45
Solvent molecules	826	859	671
Glycerol molecules	3	1	3
Mean B values (Å^2) [g]			
Protein	13.6	18.8	14.0
Ligand/ion	10.2	14.3	10.4
Solvent	27.2	33.1	27.4
Glycerol	35.4	23.9	34.8
Model r.m.s. deviations from ideality			
Bond lengths (Å)	0.008	0.010	0.008
Bond angles (°)	1.328	1.314	1.273
Chiral centers (Å^3)	0.088	0.089	0.089
Planar groups (Å)	0.008	0.008	0.007
Model validation [h]			
% Ramachandran outliers	0.13	0.13	0.13
% Ramachandran favored	97.6	97.6	98.0
% Rotamer outliers	0.61	0.97	0.78
C^β outliers	0	0	0
Clash score	1.7	2.4	2.3
PDB Accession code	6RTP	6RU9	6RUC

[a] Values in parentheses refer to the highest resolution shell; [b] $R_{work} = (\Sigma_{hkl} ||F_{obs}(hkl)| - |F_{calc}(hkl)||) / (\Sigma_{hkl} |F_{obs}(hkl)|) \times 100$ %; [c] R_{free} is calculated as above from a random sample containing 5% of the total number of independent reflections measured; [d] Maximum-likelihood estimate by PHENIX; [e] HysA (large subunit) is chain B, HysB (small subunit is chain A); [f] Including atoms in the alternate conformations of disordered groups of residues; [g] Calculated from isotropic or equivalent isotropic B-values; [h] Calculated with MolProbity.[3]

Table S3. Structural details

	WT (5JHS)	G50T	G491A1	G491S1
Ni atom [a]				
Occupancy	84%	67%	78%	86%
Sec489				
Conformer I	52%	46%	n.d.	29%
Conformer II	20%	20%	23%	18%
Conformer III	29%	34%	77%	53%
Cys75				
Not oxidized	-	16%	100%	76%
Sulfenate	38%	20%	-	2%
Sulfinate	62%	54%	-	21%
S atom [b]				
Occupancy	96%	81%	71%	83%
Proximal Cluster [c]				
[4Fe-4S]	75%	62%	75%	91%
[4Fe-4S-2O]	25%	38%	25%	9%

[a] In all crystal structures, the Ni ion was refined with partial occupancy: 67%, 78% and 86% in G50T, G491A and G491S, respectively, compared to 84% for the WT. The incomplete Ni occupancy probably results from a mismatch between the rates of recombinant protein expression and the native nickel incorporation machinery;[4] [b] the sulfur species bound to the Ni and Se in conformers I and II was refined with occupation levels of 81%, 71% and 83%, in G50T, G491A, and G491S respectively, compared to 96% for the WT; [c] unlike the oxidation of Cys75 to the sulfinate state, the partial oxidation of the proximal iron-sulfur cluster to $[Fe_4S_4O_2]$ is reversible.[5] In the previously reported WT structure the proximal iron-sulfur cluster was 25% oxidized[4] and, except for structure G491S where this oxidation level is only *ca.* 9%, comparable values are observed for the G50T and G491A structures, 38% and 25% respectively.

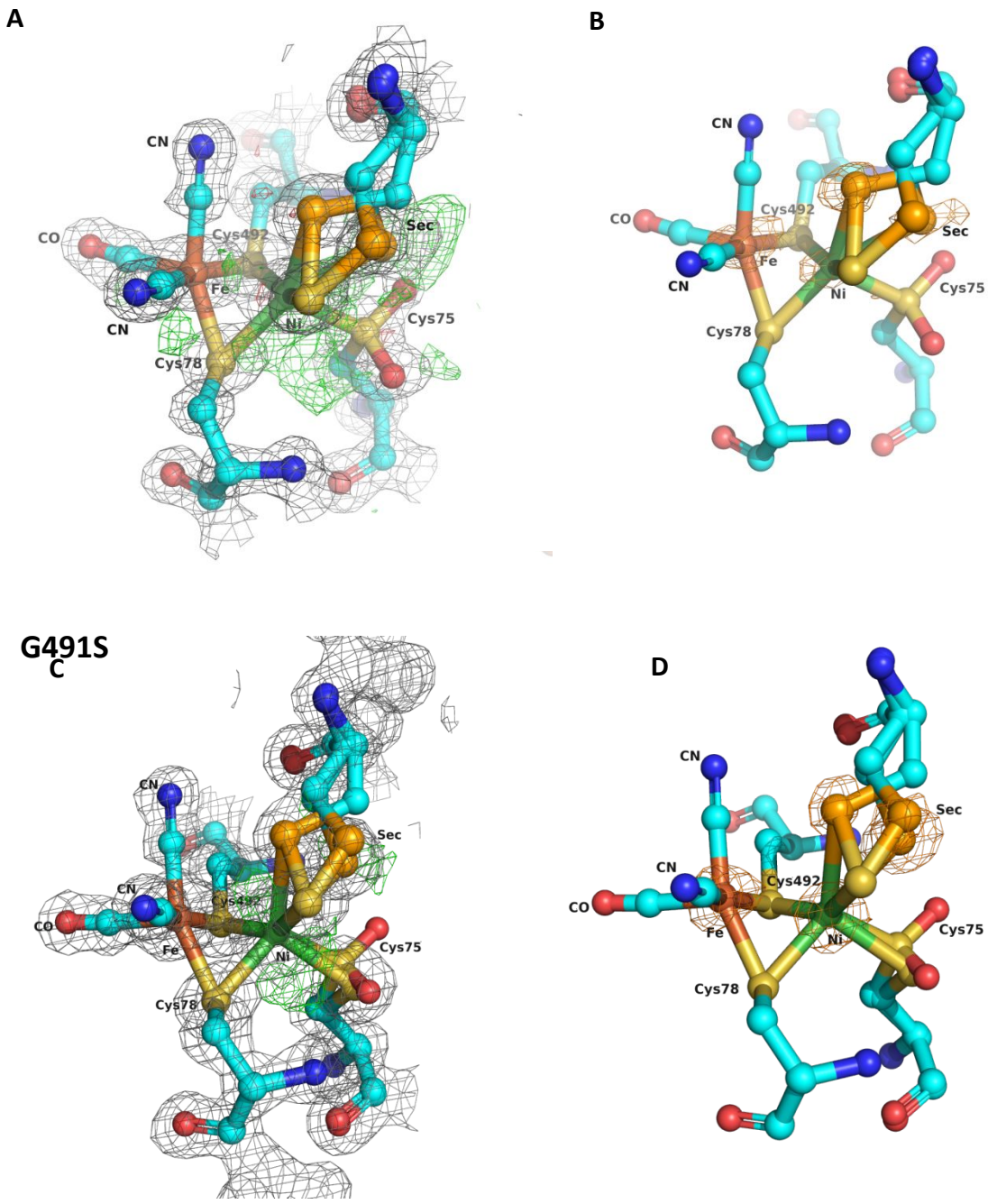

Figure S3. Active site of the aerobically purified and crystallized [NiFeSe] hydrogenase variants. (**A, C**) View of the refined structures of G50T (A) and G491S (C) with their corresponding $2|F_o|-|F_c|$ and $|F_o|-|F_c|$ maps, showing the additional Sec positions. The $2|F_o|-|F_c|$ map (gray mesh) is drawn at the 1.5 map r.m.s. level and the $|F_o|-|F_c|$ map is represented at the 3.5 (green mesh) and -3.5 (red mesh) map r.m.s. levels. (**B, D**) View of the final refined structure of G50T (**B**) and G491S (**D**) superimposed with the anomalous Fourier map (orange mesh) drawn at the 4.5 map r.m.s. level and calculated with phases from the partially refined structure represented in (a and c, respectively). The [NiFe] binuclear center and the sidechains of its protein ligands are represented in ball-and-stick and the protein chain is represented as a semitransparent cartoon. Atom colors are brown for iron, green for nickel, gold for sulfur, red for oxygen, light blue for carbon, blue for nitrogen and orange for selenium. Hydrogen atoms are omitted for clarity.

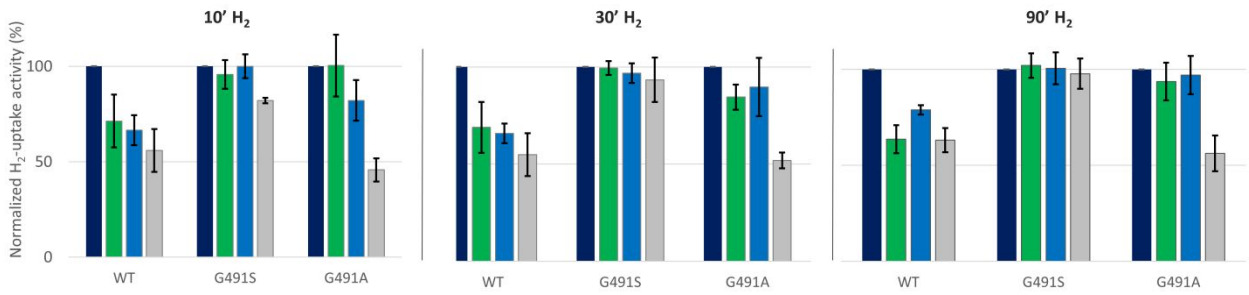

Figure S4. H_2 uptake activity of WT and variants after 1 hour (green), 4 hours (blue) and overnight (grey) exposure to air, followed by 10, 30 and 90 minutes reactivation under 0.5 atmosphere H_2. The activities were normalized by the corresponding maximum activity of each protein (dark blue), reported in Table 1. The data correspond to the average of three individual experiments, each done in triplicate and the error bars correspond to the standard deviations.

Table S4. Channels predicted by CAVER in [NiFe] and [NiFeSe] hydrogenase structures

Organism	PDB	Starting atom 1 (a)	C1	C2	Starting atom 2 [a] (a)	C1	C2
*Dv*H	5jhs	C75 Sγ	Y	Y	-	-	-
*Dv*H G50T	This work	C75 Sγ	N	Y	-	-	-
*Dv*H G491A	This work	C75 Sγ	N	N	A491 Cβ	Y	Y
*Dv*H G491S	This work	C75 Sγ	N	N	S491 Oγ	Y	Y
Dmb	4kn9	C70 Sγ	Y	N	-	-	-
*Dv*MF	4u9h	C81 Sγ	N	N	A548 Cβ	N	N
Dd	1e3d	C71 Sγ	N	N	A538 Cβ	N	N
Dg	2frv	C65 Sγ	N	N	A532 Cβ	N [b]	N [b]
Df	1yqw	C72 Sγ	N	N	A545 Cβ	N	N
Ec	6ehq	C61 Sγ	N	N	A548 Cβ	N	N
Av	3myr	C61 Sγ	N	N	A557 Cβ	N	N
Cs77	5xvb	C61 Sγ	N	N	S548 Oγ	Y	N
Ec	5a4f	C76 Sγ	N	N	A578 Cβ	N	N
Re	3rgw	C75 Sγ	N	N	A599 Cβ	N	N
Hm	3ayx	C76 Sγ	N	N	A592 Cβ	N	N

[a] Both residues are in the large subunit. The second starting atom is explored in instances where the first atom yields a negative result; [b] a tunnel system with 5 branches appears in this calculation, matching the hydrophobic tunnel system.

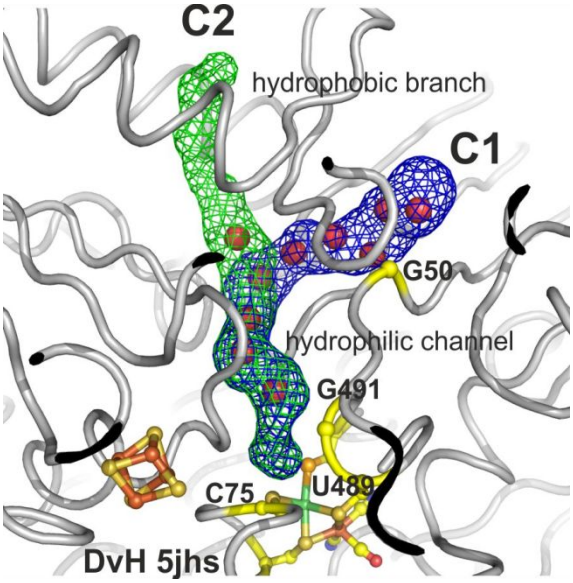

Figure S5. The hydrophilic channel (C1) and hydrophobic side-channel (C2) referenced in Table S4.

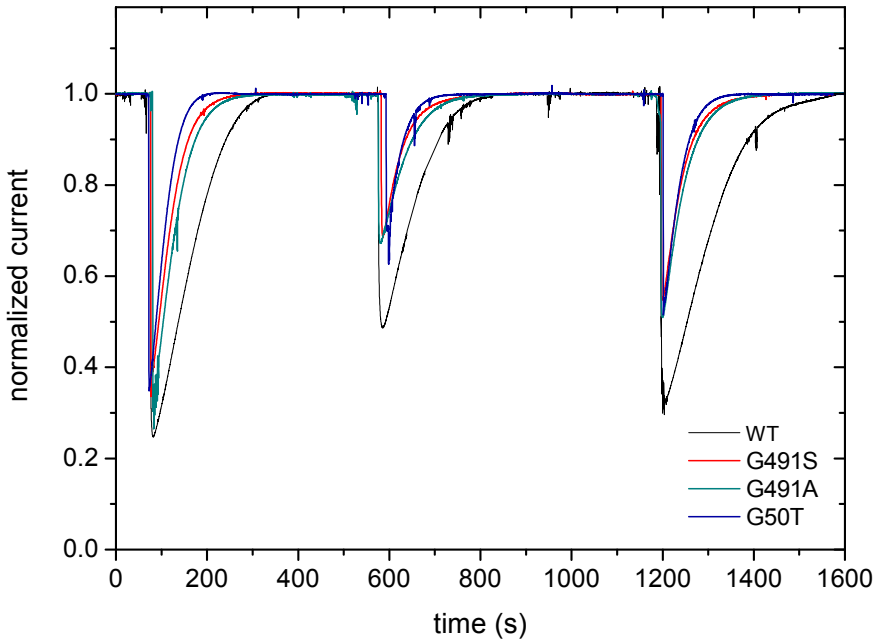

Figure S6. Effect of CO on the H_2 oxidation current of WT [NiFeSe] hydrogenase and variants adsorbed onto a graphite rotating electrode. Experimental conditions: [CO] = 4, 1, 2 μM, E= -0.060 V vs. SHE, 1 bar H_2, pH 7, T= 40°C, electrode rotation rate = 3000 rpm.

References

(1) Diederichs, K.; Karplus, P. A., Improved R-Factors for Diffraction Data Analysis in Macromolecular Crystallography. *Nat. Struct. Biol.* **1997**, *4*, 269–275.

(2) Matthews, B. W., Solvent Content of Protein Crystals. *J. Mol. Biol.* **1968**, *33*, 491–497.

(3) Chen, V. B.; Arendall, W. B.; Headd, J. J.; Keedy, D. A.; Immormino, R. M.; Kapral, G. J.; Murray, L. W.; Richardson, J. S.; Richardson, D. C.; Richardson, D. C., MolProbity: All-Atom Structure Validation for Macromolecular Crystallography. *Acta Crystallogr. Sect. D Biol. Crystallogr.* **2010**, *66*, 12–21.

(4) Marques, M.; Tapia, C.; Gutiérrez-Sanz, Ó.; Ramos, A. R.; Keller, K. L.; Wall, J. D.; De Lacey, A. L.; Matias, P. M.; Pereira, I. A. C., The Direct Role of Selenocysteine in [NiFeSe] Hydrogenase Maturation and Catalysis. *Nat. Chem. Biol.* **2017**, *13*, 554–550.

(5) Marques, M.; Coelho, R.; Pereira, I. A. C.; Matias, P. M., Redox State-Dependent Changes in the Crystal Structure of [NiFeSe] Hydrogenase from Desulfovibrio Vulgaris Hildenborough. *Int. J. Hydrogen Energ.* **2013**, *38*, 8664–8682.